

Autoresonant vibro-impact system with electromagnetic excitation

I.J. Sokolov, V.I. Babitsky*, N.A. Halliwell

Wolfson School of Mechanical and Manufacturing Engineering, Loughborough University, Leicestershire LE11 3TU, UK

Accepted 2 April 2007

The peer review of this article was organised by the Guest Editor

Available online 4 June 2007

Abstract

Vibration is often used to improve the performance of material handling, processing or separation machinery. Linear suspension and sinusoidal motion of moving parts are usually employed in the design of these machines. A typical example would be vibrating screens used to grade gravel in sand and gravel extracting systems. A dramatic improvement in performance can be achieved if nonlinear suspension, with limiters to provide a vibro-impact motion, can be established. Unfortunately, effective vibro-impact resonant behaviour cannot be sustained in practice with traditional forced excitation due to the system sensitivity to small changes in load. Effective vibro-impact regimes, however, can now be achieved using the concept of autoresonant systems. An electromagnetic drive actuator is a simple and reliable means of vibration excitation. Importantly, this drive allows for an expansion of the autoresonant approach towards high-power applications. This paper introduces a novel autoresonant machine design, which has been developed for this type of actuator. Autoresonant operation is demonstrated using an experimental rig of vibro-impact shale shaker with electromagnetic actuator.

© 2007 Elsevier Ltd. All rights reserved.

1. Introduction

Vibrating systems in technology: A variety of processing machines deliberately uses vibration [1]. In some machines, such as vibratory conveyors, vibration provides the working process. In others application of vibration results in significant improvement in their performance (hoppers, sieves, compactors, etc.). In some screening machines, vibration is used to assist both the process of transportation of mixture along the screen and process of separation of the mixture. A shale shaker is an example of such machine. It is used in the extractive technology to separate special drilling liquid (“mud”) and drilled solids [2].

The majority of these machines have similar features:

- the working frequency is well above the resonant one,
- linear suspension is used,
- the vibrating part performs sinusoidal (reciprocating or circular/elliptical) motion.

*Corresponding author. Tel.: +44 1509 227503; fax: +44 1509 227502.

E-mail address: V.I.Babitsky@lboro.ac.uk (V.I. Babitsky).

There are important reasons for these features. Although the resonant regimes are most effective [3,4], they are usually avoided (even in linear systems) because of difficulties of the regime maintenance. This problem is most critical in systems with high Q -factor or varying parameters. Furthermore, the Sommerfeld effect [5] makes resonant regimes practically inapplicable, when an asynchronous drive with limited power supply is used for excitation. In systems with nonlinear suspension and traditional excitation the resonant regimes cannot be used, in practice, due to jump phenomenon even in the case when a synchronous drive or drive with unlimited power is employed [5,6].

Nonlinear systems: Nonlinearity can be either a natural feature of suspension or the result of a specific design feature of the vibrating machine. For example, air springs are nonlinear by nature. Any limiters designed to restrict amplitude of vibration introduce nonlinearity into suspension even if linear springs are used. In some cases, the deliberate employment of nonlinear suspension may produce fundamentally new characteristics in the machine behaviour. Vibration becomes non-sinusoidal. This can be used to bring asymmetry into vibration of the operating element. Such asymmetry can improve performance of vibratory conveyors [1]. Nonlinearity can essentially change parameters of vibration as this happens when impacts are added to traditional sinusoidal vibration.

Vibro-impact motion: A vibro-impact system [7] is the particular case of a system with nonlinear elasticity and damping. Compared to the linear system, the peak values of acceleration in the vibro-impact system can be considerably higher at the same frequency and amplitude of vibration. Fig. 1(a) shows a simple model of a vibro-impact system with elastic limiters. Fig. 1(b) illustrates, how the displacement, velocity and acceleration of vibrating body change under successive addition of two asymmetric elastic limiters 1 and 2 to the simple vibrating system. These diagrams are plotted for system with constant energy and without dissipation.

The initial parts of the diagrams correspond to sinusoidal impact-free vibration of initial mass–spring system without limiters. Then elastic limiter 1 has been added to the system at the time instant t_1 . The next interval (t_1, t_2) illustrates vibration of the system with one limiter. Then elastic limiter 2 has been added at the time instant t_2 . The final parts of the diagrams show vibration of the system with two limiters and two impacts per a period.

Hence, impacts can essentially increase the peak values of acceleration and can bring an asymmetry to the vibration. It may be suggested that these features of vibro-impact motion can improve the performance of some vibrating machines. Screening machines are of particular interest, especially if liquid and solids are separated. When the screen moves downwards, high peak values of acceleration caused by impacts against the lower limiter can improve the liquid flow rate through the screen and increase the dryness of solids discharged. When the screen moves upwards, additional weak impacts against the upper limiter can decrease mesh blockages and facilitate the process of transportation along the screen.

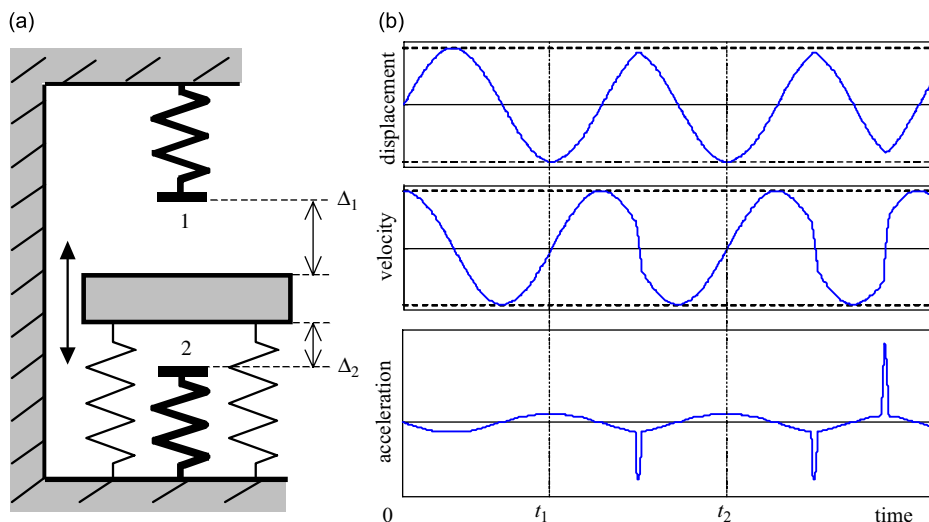


Fig. 1. Simple vibro-impact system with asymmetric elastic limiters (a) and corresponding waveforms (b) of vibration.

Practical application of vibro-impact systems is a major challenge using traditional means of excitation. Fig. 2(a) and (b) shows the known amplitude–frequency curves for vibro-impact systems with one limiter and two rigid asymmetric limiters, respectively [7].

These curves are ambiguous and the lower parts of resonant peaks shown with dashed lines correspond to regimes that are unstable and cannot be obtained under conventional forced excitation. The horizontal dashed and dash–dotted parts of the curve in Fig. 2(b) are arbitrarily drawn separately, though in fact they coincide. The instability results in jump phenomenon [6]. This effect is typical for nonlinear systems. The jumps are shown with thin vertical dashed lines. The jumps take place as the frequency of excitation is slowly increased or decreased. The dotted parts correspond to nonperiodic regimes with weak impacts [7]. The dash–dotted parts of curves between the vertical lines (jumps) correspond to theoretically stable periodical regimes with strong impacts. It is in these regimes that impacts are substantial. However, these regimes cannot be practically used under forced excitation for two reasons. First, they can only be reached by means of a slow increase in frequency from an initial value below the left vertical line. Otherwise, the low-amplitude mode without impacts (the lower solid branch of the curves) will be obtained. Second, the jump phenomenon takes place in these regimes under accidental disturbance that again results in low-amplitude vibration without impacts.

Auto-resonant excitation is the method that enables us not only to overcome the above difficulties but also to maintain the most effective resonant regime under variable load and other parameters.

Auto-resonant excitation: The new approach was recently developed to design resonant vibratory equipment as a *self-sustained* oscillating system with electronic and electro-mechanical feedback using an actuator of the synchronous type.

Synchronous actuators produce an excitation force, whose frequency does not depend on load, but only on the frequency of the power supply. For such actuators, the resulting force of excitation has exactly the same frequency as the power supply. The feedback in such a system produces the excitation force F by means of transformation of the displacement (velocity, acceleration) signal [3,4].

The feedback in its simplest form (Fig. 3(a)) shifts the phase of the vibration signal from the sensor and amplifies its power (usually with limitation). This signal feeds the actuator, which transforms it to an excitation force. Such a system does not include an external source of the excitation frequency. The frequency and the amplitude of vibration depend on parameters of the mechanical system and the feedback circuit. Under a certain phase shift in the feedback circuit the resulting vibration has the same frequency as the natural frequency of the mechanical subsystem without feedback, i.e. the regime is resonant. The regime can be controlled by means of changing the phase shift [8], whereas changing the level of amplitude limiting in the feedback circuit also allows control the amplitude of vibration. If we consider harmonic self-sustained vibration of a simple single-degree-of-freedom system with phase control and harmonic excitation, it is obvious, that the resonant regime takes place when the force is in phase with the vibratory

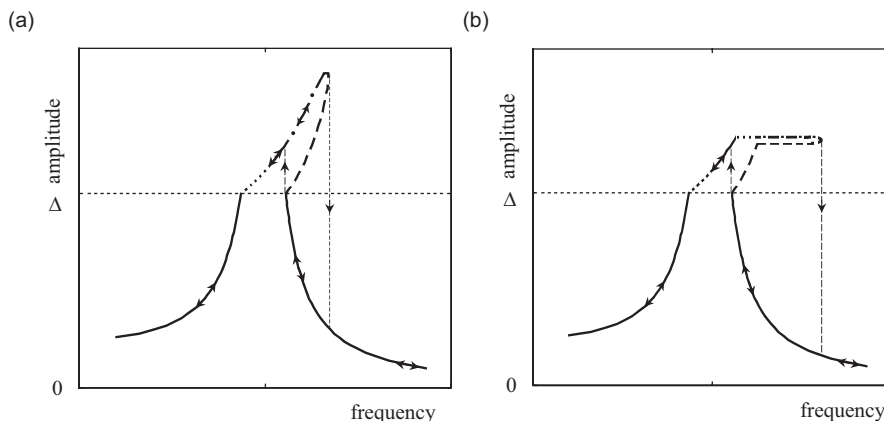


Fig. 2. Amplitude–frequency curves for vibro-impact systems with one limiter (a) and two limiters (b).

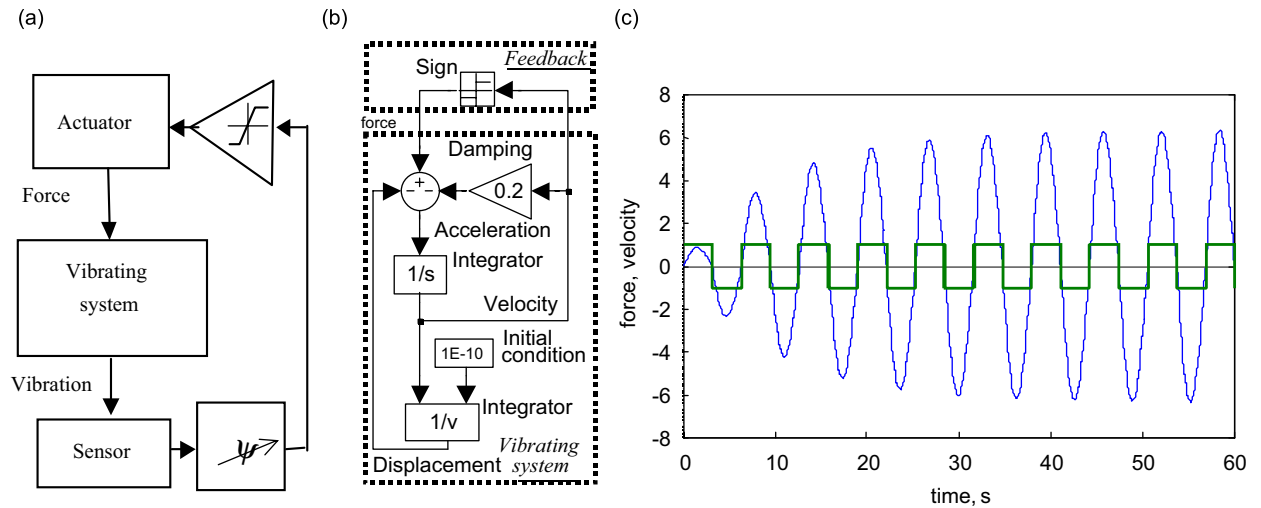


Fig. 3. Autoresonant system: feedback design (a), computer model (b) and behaviour (c).

velocity (or lags $3\pi/2$ in phase from the vibratory displacement). This system is designated as an *autoresonant* one [3,4]. It keeps the resonant regime of oscillation when the natural frequency of the mechanical subsystem changes. Effectiveness of the autoresonant excitation relies on a specific geometry of amplitude–phase characteristics of the vibration system. Properties of the amplitude–phase curves differ essentially from properties of known amplitude–frequency (resonant) curves for many systems of practical interest [8]. These curves are usually single valued and gently sloping near the resonance. That is why resonant vibration is stable under autoresonant excitation and such a system does not need precise tuning of the phase to maintain the resonant regime, in contrast with traditional forced excitation with frequency control.

If damping is not extremely high in a vibrating system, such a system exhibits filtering properties. Those harmonics of excitation that are close to natural (resonant) frequencies of the system prevail over all other harmonics in the resulting vibration. Owing to these filtering properties we usually do not need strictly sinusoidal excitation to get resonant vibration. In practice, an arbitrary shape of excitation with pronounced first harmonics is appropriate for the autoresonant system. This is especially important in nonlinear autoresonant systems, where vibration itself can be non-harmonic, and in powerful systems, where it is often difficult to produce a harmonic excitation force.

The elementary Matlab–Simulink computer model of an autoresonant system is shown in Fig. 3(b). Here, a rectangular pulse force is used for excitation, the velocity signal is used in the feedback circuit. There is no need for any special phase-shifting element to provide resonant mode of vibration in this system. Fig. 3(c) illustrates the model behaviour.

Electromagnetic actuator: In this paper, only elemental electromagnetic actuators are considered (as distinct from electric motors that also are in fact electromagnetic drives). The simplicity and reliability of an electromagnetic drive makes it one of the most promising vibratory actuators [1]. An electromagnetic actuator does not have friction and wear; it does not need moving seals, it is maintenance free and silent. However, as a result of some features, electromagnetic actuators do not have a wide use in industry compared with common rotary actuators.

The electromagnetic exciter is only capable of producing an attracting force proportional to the squared electric current. This results in the two features that must be taken into consideration when designing such an actuator.

Firstly, for the full-wave magnet shown in Fig. 4(a), the exciting force has the doubled frequency of the alternating voltage supply. Fig. 4(b) demonstrates the corresponding waveforms of steady-state voltage U , current I and attracting force under alternating sinusoidal voltage supply. In case of the half-wave magnet the alternating voltage feeds it through a half-wave diode rectifier, as shown in Fig. 5(a). In this case the resulting

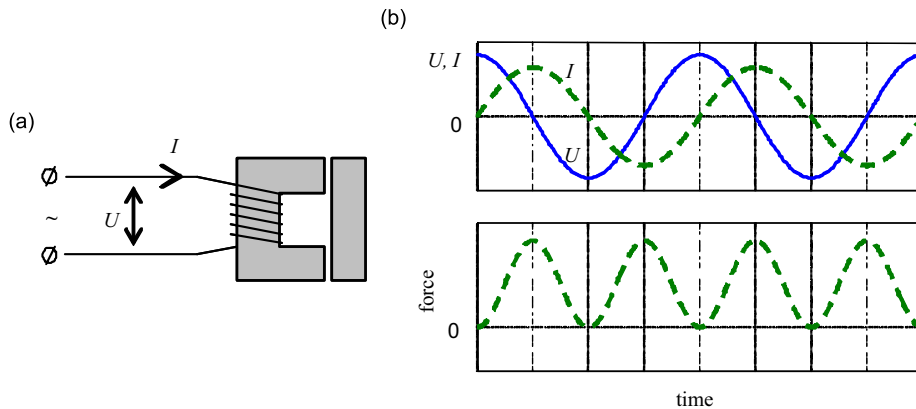


Fig. 4. Full-wave electromagnetic vibrator (a) and corresponding waveforms (b) of steady-state voltage U , current I and attracting force under sinusoidal voltage supply.

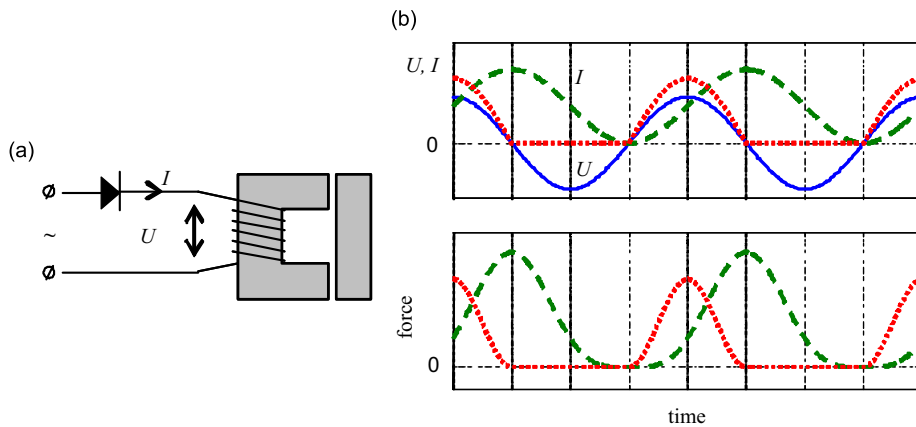


Fig. 5. Half-wave electromagnetic vibrator (a) and corresponding waveforms (b) of steady-state voltage U , current I and attracting force under sinusoidal voltage supply.

attracting force is not sinusoidal, as it is shown with dashed line in Fig. 5(b),¹ has a pronounced main harmonic with the same frequency as the supply voltage. Hence, only the half-wave magnet is an actuator of the synchronous type and can be used in autoresonant machines.

Secondly, the excitation force has necessarily a constant component commensurable with the amplitude of the alternating component. The electromagnetic exciter has a high mass-to-force ratio in comparison with other types of actuators. This ratio is limited by heating. Hence, the problem of heat emission is very important, and the constant component of current should be minimised in order to reduce heating.

High inductance is the other feature of the electro-magnet actuator. Special measures should be taken to protect electronic switches when using or designing powerful electric generators to feed such an actuator. If contact switches are used, for example, in some self-sustained systems, contacts can deteriorate very fast as a result of the high inductance of the load. This problem is especially prevalent in high-power applications.

Different designs of linear electromagnet drives exist with different types of tractive characteristic [9]. For the most common design shown in Fig. 6(a), this characteristic is essentially nonlinear. In theory, the

¹It is interesting to note that usually the shape of current and force in the half-wave magnet is believed to be as shown with dotted line in Fig. 5(b) (see, for example, Ref. [1, p. 92]). These shapes are correct, however, only in the case when the Ohmic resistance considerably exceeds the inductive reactance, which usually does not take place for electromagnetic vibrators.

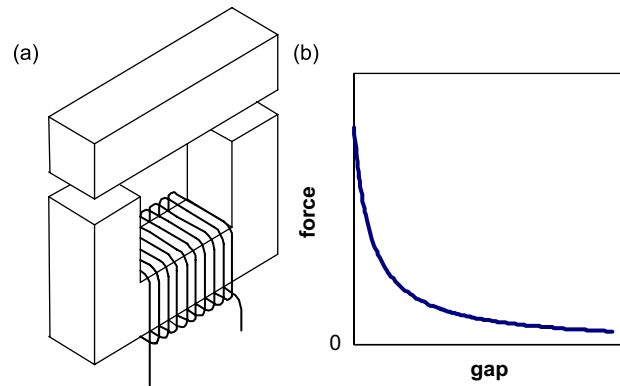


Fig. 6. Common design of electromagnetic vibrator (a) and its tractive characteristic (b).

attracting force is approximately inversely proportional to the gap between the armature and the core under constant electric current as shown in Fig. 6(b).

These tractive characteristics produce the following features in an electromagnetic vibrators application:

- Working clearance between core and armature must be as small as possible. Otherwise, big currents are necessary to produce reasonable force. This makes employment of electromagnetic vibrators difficult when the gap or vibration amplitude can significantly vary due to changing load.
- The common over-resonant regime of vibration is the most inefficient for these vibrators. As the displacement changes in antiphase to the excitation force in such regimes, the maximum force corresponds to the maximum gap, when the magnet transforms the maximum current to the force least efficiently.

The last two features account for common application of electromagnetic actuators in resonant vibrating machines [1] that need relatively small forces for excitation. These vibrators could be also effectively employed in nonlinear or vibro-impact machines with elastic or rigid limiters. Such limiters prevent impacts between armature and core and therefore allow for the use of small gaps. However, both the resonant and the vibro-impact regimes are very rarely employed in conventional vibratory machines, as previously explained.

All these features of electromagnetic exciters restrict their wide use in conventional vibrating machines. An autoresonant approach provides new possibilities for wide industrial application of the electromagnetic actuators because the optimal combination of resonant regime and nonlinear suspension with limiters can be effectively used.

2. Electromagnetic actuator for autoresonant system

In this section, different schemes of electromagnetic vibrators are considered in order to choose the most efficient scheme for a high-power autoresonant machine.

As mentioned above, a full-wave electromagnet cannot be used in autoresonant applications as it produces a force with a doubled frequency. Only a half-wave electromagnet can be used in the autoresonant system. Such a magnet is usually connected to the sinusoidal alternating voltage through rectifying diode or thyristor as shown in Fig. 5(a). Usually, the inductive reactance of the coil is much higher than its ohmic resistance at the working frequency. In this case, the magnet steady-state voltage, current and force waveforms under sinusoidal supply voltage are shown in Fig. 5(b). The force (dominant harmonic) and the voltage have the same frequency; the force has a $\pi/2$ lag in phase with respect to the voltage. The only but important disadvantage of such a scheme is that the current has the constant component proportional to the amplitude of the alternating component.

The common tandem design, shown in Fig. 7(a), removes the constant component of the total excitation force produced by two magnets.

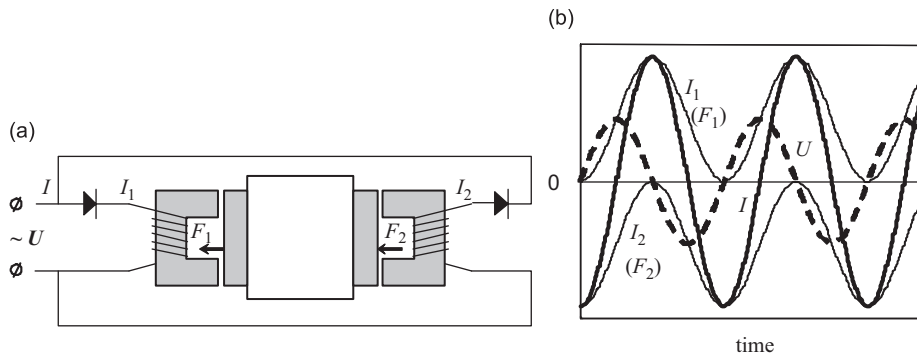


Fig. 7. Tandem design of electromagnetic vibrator (a) and corresponding waveforms (b) of voltage U , currents I_1 , I_2 , I and forces F_1 , F_2 .

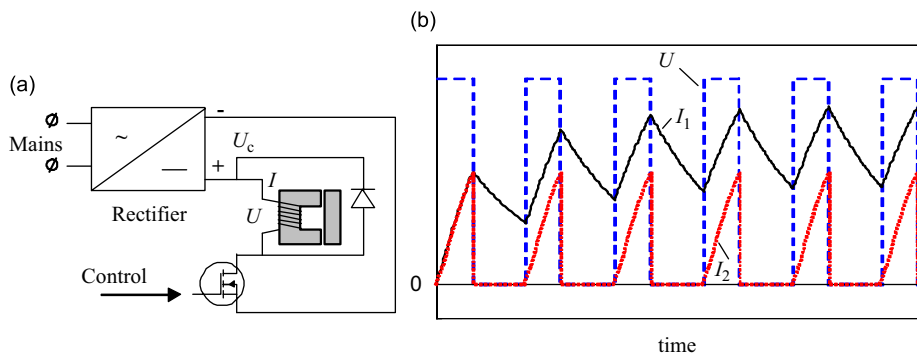


Fig. 8. Simplest scheme of electromagnetic vibrator with rectifier and switch (a) and corresponding waveforms (b) of voltage U and current I .

The currents waveforms under sinusoidal supply voltage U are shown in Fig. 7(b). The total current I also does not have a constant component. However, this design is not the most efficient as the current is wasted partly to produce opposite forces F_1 and F_2 acting simultaneously at each instant of time. Hence, a part of the total current heats the coils without producing a useful force.

It was mentioned in the introduction that the autoresonant system does not need harmonic excitation and usually requires the excitation force amplitude to be limited. Hence, it is tempting to use a simple rectifier as a source of constant voltage U_c and power semiconductor switches instead of linear amplifier.

However, the simplest scheme with one electronic switch and freewheeling diode shown in Fig. 8(a) is not appropriate because it results in a constant component of the resulting current I_1 which is higher than the alternating component, as shown in Fig. 8(b), if the ohmic resistance of the coil is small. Hereafter, the popular MOSFET transistor is used as a switch, though other types can be employed.

The high constant component of current can be avoided by removing the diode (dotted line in Fig. 8(b)). However, in this case an extremely high back voltage is applied to the switch at the instants of disconnection as a result of the high inductance of the coil.

The common scheme of inverter shown in Fig. 9(a) can be employed to convert the d-c voltage U_c to the alternating square-wave voltage U . Here, pairs of switches 1&4 and 2&3 work simultaneously one pair after another.

Fig. 9(b) shows the corresponding voltage and currents waveforms. This scheme is more promising, but is not the most efficient solution for a high-power autoresonant system since it has the same disadvantage as scheme shown in Fig. 7. It produces opposing forces, which act simultaneously at each instant of time, and hence lacks efficiency in terms of heat emission. In addition, switch timing is highly critical. The time interval between switching on one pair of switches and switching off the other pair must be zero. Even small variations

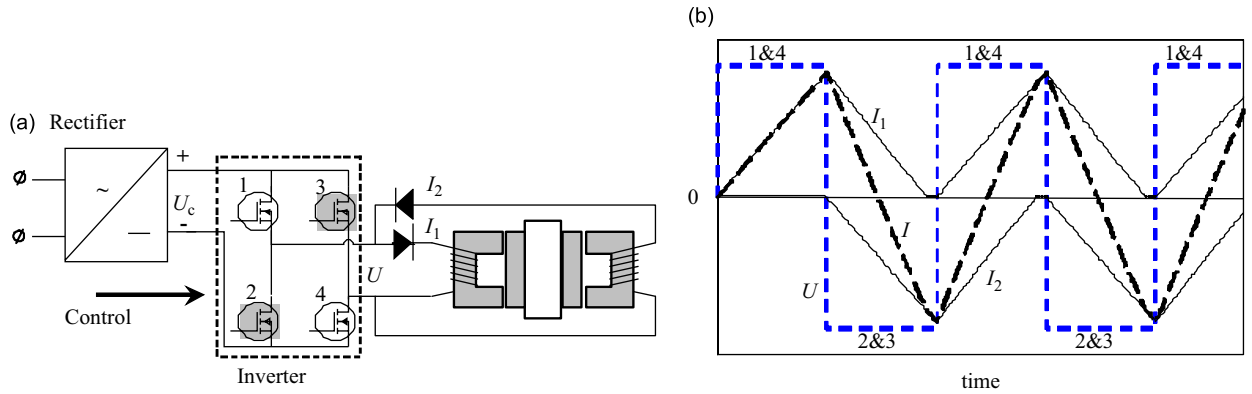


Fig. 9. Common scheme of electromagnetic vibrator with inverter (a) and corresponding waveforms (b) of voltage U and currents I_1, I_2, I .

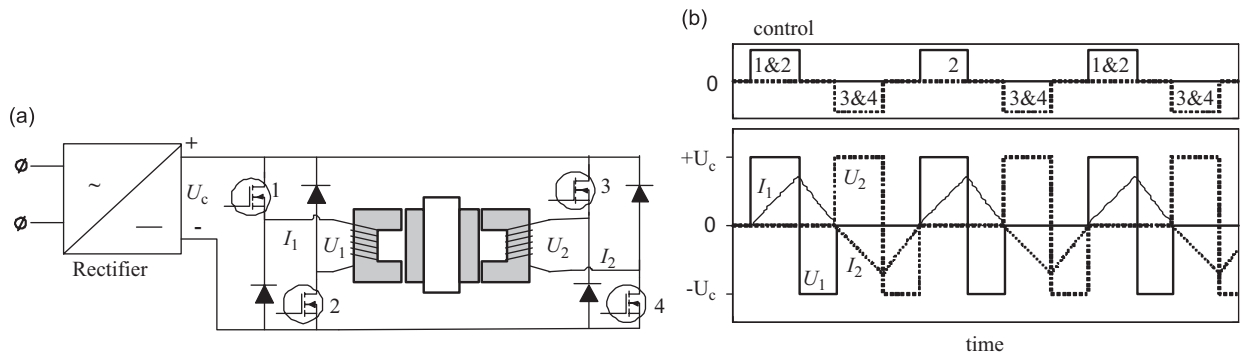


Fig. 10. Scheme of electromagnetic vibrator with independent control of magnets (a) and corresponding waveforms (b) of control signal, voltages U_1, U_2 and currents I_1, I_2 .

of this interval in both directions can result in either a short circuit (if both pairs are switched on simultaneously for a short time) or high back voltage applied to switches (if both pairs are switched off simultaneously for a short time).

The solution that we think is the most efficient is shown in Fig. 10(a). This scheme allows independent control of each magnet and is free of the above drawbacks. It naturally uses inductance of coils to produce the desired waveforms of currents while high back voltages are never applied to switches and switching timing is not highly critical. Both switches in each pair 1&2 and 3&4 are turned on or off simultaneously. The positive voltage $+U_c$ is applied to the coil when both corresponding switches are turned on. Otherwise the opposite voltage $-U_c$ is applied until the current drops to zero.

Importantly, this scheme does not produce opposing forces under the proper control shown in Fig. 10(b). Here, the upper diagram represents the time chart of control: the positive pulses switch on the first pair of switches (1&2); the negative pulses switch the other pair (3&4) on. The lower chart in Fig. 10(b) shows the corresponding waveforms for the magnets voltages and currents. The I_2 current is arbitrarily shown negative to reflect the opposite direction of the force it produces. Changing the constant voltage U_c or the on–off time ratio (pulse duration to its period) of the control signal can control the amplitude of both the current and excitation force. The voltage applied to the switches never exceeds U_c . It is worth noting that in the last two schemes described the dc power supply (rectifier) must allow a short-time reverse current.

3. Control system

The aim of the autoresonant control system is to transform the vibration transducer signal shown in Fig. 1(b) to the proper control signal shown in Fig. 10(b). The control must provide for effective operation of the

electromagnetic exciter and a certain phase shift between resulting excitation force and original signal of vibration. These conditions must be satisfied under changing frequency and amplitude of vibration. Unlike conventional resonant machines with frequency control, an autoresonant system usually does not need the phase shift in the feedback circuit to be precisely maintained in order to ensure resonant operation [8].

One of the possible ways of transformation is shown in Fig. 11(a). This uses both displacement and velocity signals to produce the control signal. The average value x_{av} of the displacement is also used (dash-dotted bold line in the upper diagram).

The average value generally differs from zero (equilibrium position) for vibration with asymmetric limiters. Fig. 12 illustrates this using an example of a system with rigid limiters; the average value is shown with dashed line. It remains zero for low-amplitude vibration without impacts, then grows along with amplitude for vibration with one-sided impacts, then remains approximately constant for vibration with two-sided impacts.

The lower diagram in Fig. 11(a) shows the waveforms of currents in two magnets providing that the armature is stationary. The real currents waveforms may slightly differ from shown in this figure due to armature vibration. The force waveform (not shown) will also reflect the nonlinear transformation of the current to the attraction force. However, it is clear that a fundamental harmonics of resulting current and force are *approximately* in phase with the velocity or lags 3/4 of the period from the displacement. As explained in the introduction, this phase relation corresponds to the resonant vibration. It will be shown below that this means of control results in a regime of vibration, which is very close to the most intensive autoresonant one. Hence, the feedback does not need an additional phase-shifting element. The above algorithm of transformation can be achieved in practice by means of simple electronic components. It does not need two sensors; one displacement or velocity transducer is sufficient. The second necessary signal can be obtained by integration or differentiation.

The on–off time ratio of the control signal in Fig. 11(a) corresponds to the most efficient regime of the electromagnetic actuator. For given value of the constant voltage supply the amplitude of current is the maximum possible value under which opposing excitation forces do not act simultaneously.

If necessary, the amplitude of vibration can be controlled either by changing the constant supply voltage U_c or by changing the on–off time ratio of the control signal. In practice, the latter method is more suitable. The current (and amplitude) can be reduced by a reduction in the value of the on–off ratio. To do this, two different signals $x_{av} \pm kX$ can be used instead of x_{av} as shown in Fig. 11(b). Here, X is the amplitude of

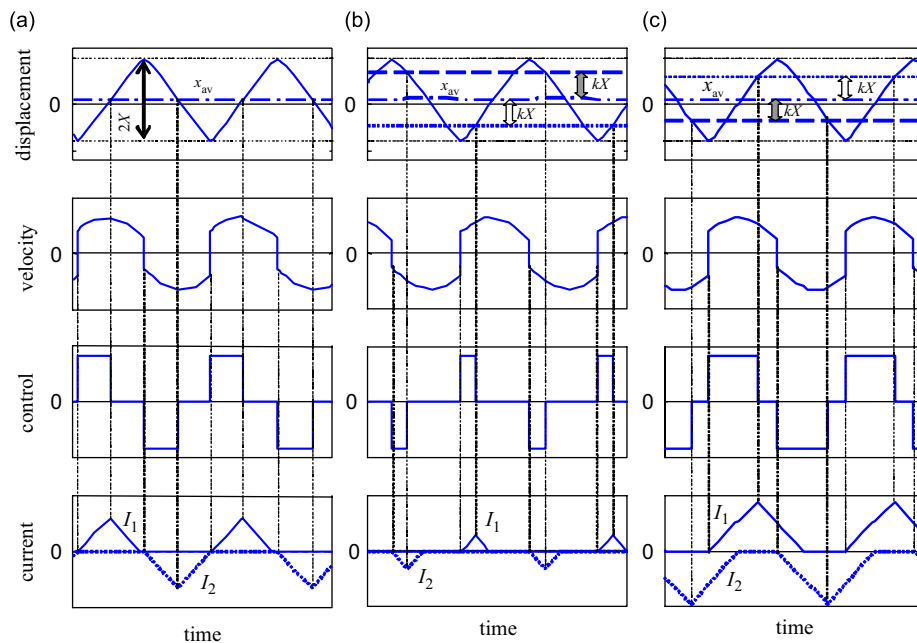


Fig. 11. Transformation of vibration signal to control signal and currents (a) and control of the currents amplitude (b, c).

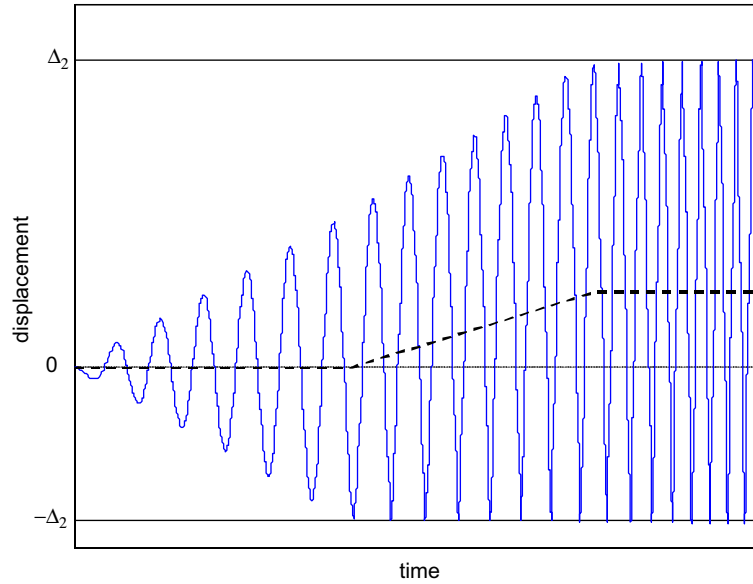


Fig. 12. Average value of displacement in vibro-impact system with asymmetric rigid limiters.

vibration and k is a constant coefficient: $0 \leq k \leq 1$. The on–off time ratio and current can be also increased the same way as shown in Fig. 11(c). Although this results in an increase in the currents and force amplitude this regime is less efficient due to opposing forces acting during part of period. This method of the current control has a side effect of slightly changing the phase relation between the vibration and force. However, it was mentioned above and will be demonstrated below that an autoresonant regime has a very low sensitivity to variation in the phase shift provided by the feedback circuit. The general mathematical expression for the above algorithm of the displacement x and the velocity \dot{x} transformation to the control signal u is as following:

$$u = \{[\dot{x} > 0] \text{ AND } [x < (x_{av} - kX)]\} - \{[\dot{x} < 0] \text{ AND } [x > (x_{av} + kX)]\}, \quad -1 \leq k \leq 1. \quad (1)$$

The amplitude and average values of currents in the coils are approximately proportional to the period of vibration. To avoid extremely high currents under low frequency of vibration the duration of the control pulses shown in Fig. 11 can be limited to a maximum value. This limitation will act only at low frequency.

4. Mathematical model and computer simulation

4.1. Mathematical model

The electro-mechanical model shown in Fig. 13 was used for design of the experimental rig of the vibro-impact shale-shaker. The machine has one mechanical degree of freedom, a tandem electromagnetic actuator and two asymmetric limiters. The total mass of all moving parts is m . Spring and damper are linear with stiffness and damping coefficients c and b , respectively. The limiters are placed with initial gaps Δ_1 and Δ_2 and bring the strong nonlinearity to the suspension. The limiters are considered as rigid and hence, impacts with them can be considered as instantaneous. They are characterised here by the restitution coefficient

$$r = -\dot{x}_+ / \dot{x}_-, \quad (2)$$

where \dot{x}_+ and \dot{x}_- are post-impact and pre-impact velocity of the vibrating body.

Fig. 13 shows the equilibrium position. The gaps in the magnets between armature and core in this position are δ_1 and δ_2 . It is assumed $\delta_1 > \Delta_1$ and $\delta_2 > \Delta_2$, that excludes collisions between armatures and cores. Both electromagnets are identical.

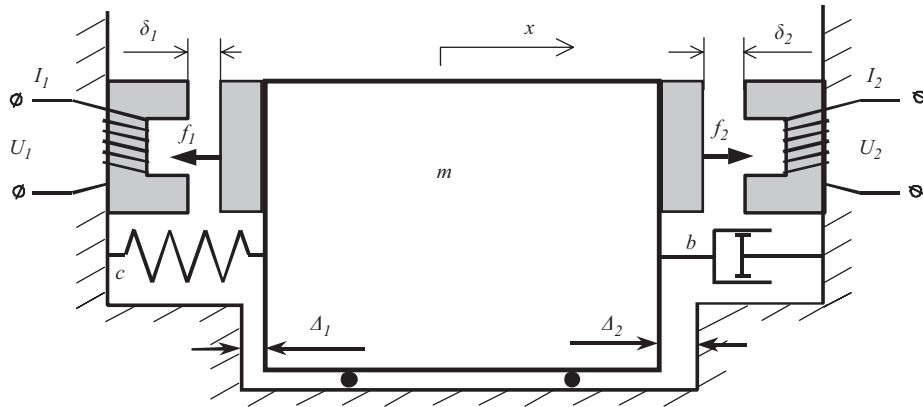


Fig. 13. Model of vibro-impact system with tandem electromagnetic actuator.

The following differential equation governs the mechanical motion of this system:

$$m\ddot{x} + b\dot{x} + cx = f_2 - f_1, \tag{3}$$

where x is the displacement of the moving part. The forces of magnetic attraction f_1 and f_2 for unsaturated magnetic system are given by [9]

$$f_1 = \frac{I_1^2}{2} L'(\delta_1 + x), \quad f_2 = \frac{I_2^2}{2} L'(\delta_2 - x), \tag{4}$$

where I_1 and I_2 are electric currents in the corresponding coils; $L'(z) = dL(z)/dz$; $L(z)$ is the inductance of the magnet's coil as a known function of the gap between the core and the armature.

The following nonlinear differential equations describe the electric currents:

$$\begin{aligned} \dot{I}_1 L(\delta_1 + x) + \dot{x} I_1 L'(\delta_1 + x) + (R + \rho(I_1)) I_1 &= U_1, \\ \dot{I}_2 L(\delta_2 - x) - \dot{x} I_2 L'(\delta_2 - x) + (R + \rho(I_2)) I_2 &= U_2, \end{aligned} \tag{5}$$

where U_1 and U_2 are the voltages applied to the correspondent coils, R is the Ohmic resistance of the coils, $\rho(I)$ is the resistance of a diode:

$$\rho(I) = \begin{cases} 0, & I \geq 0, \\ \infty, & I < 0. \end{cases} \tag{6}$$

Eqs. (3)–(6) were used for a numerical computer simulation of the electro-mechanical processes in the system. These equations describe the continuous motion between impacts or without impacts. They do not take impacts into account. Eq. (2) in the form of $x_+ = -rx_-$ comes into effect at the instants when x reaches $+\Delta_2$ or $-\Delta_1$ values. The velocity function is discontinuous at these time points. A stitching procedure [7] was used to get the full process.

The waveforms of the voltages U_1 and U_2 correspond to ones shown in Figs. 10(b) and 11(a). These voltages are a function of the control signal. Two regimes were considered: autoresonant vibration and traditional forced vibration. Control signal formation in the autoresonant system was shown in Fig. 11(a). The same electromechanical system under conventional forced excitation with frequency control was considered in order to compare its properties with the autoresonant system. In this case, an independent external frequency-regulated sinusoidal signal was used instead of the vibration signal to produce the control signal.

The MATLAB-SIMULINK software was used for computer simulation of the above mathematical model. The aggregative SIMULINK scheme is shown in Fig. 14. The bold lines with arrows in this scheme represent the vector (x, \dot{x}) signal. The ‘Control’ block has an additional input, which will be discussed below.

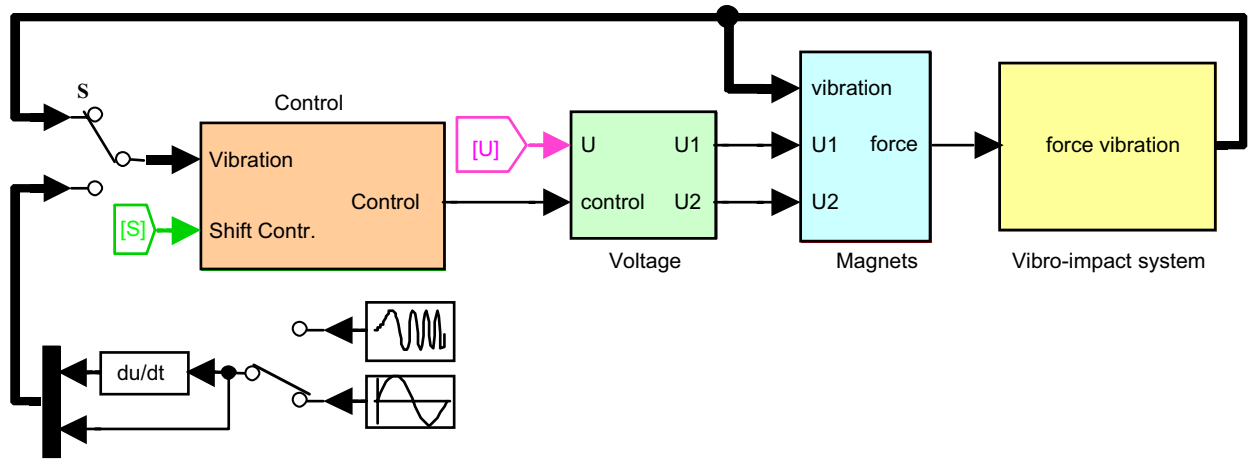


Fig. 14. Aggregated MATLAB-SIMULINK computer model.

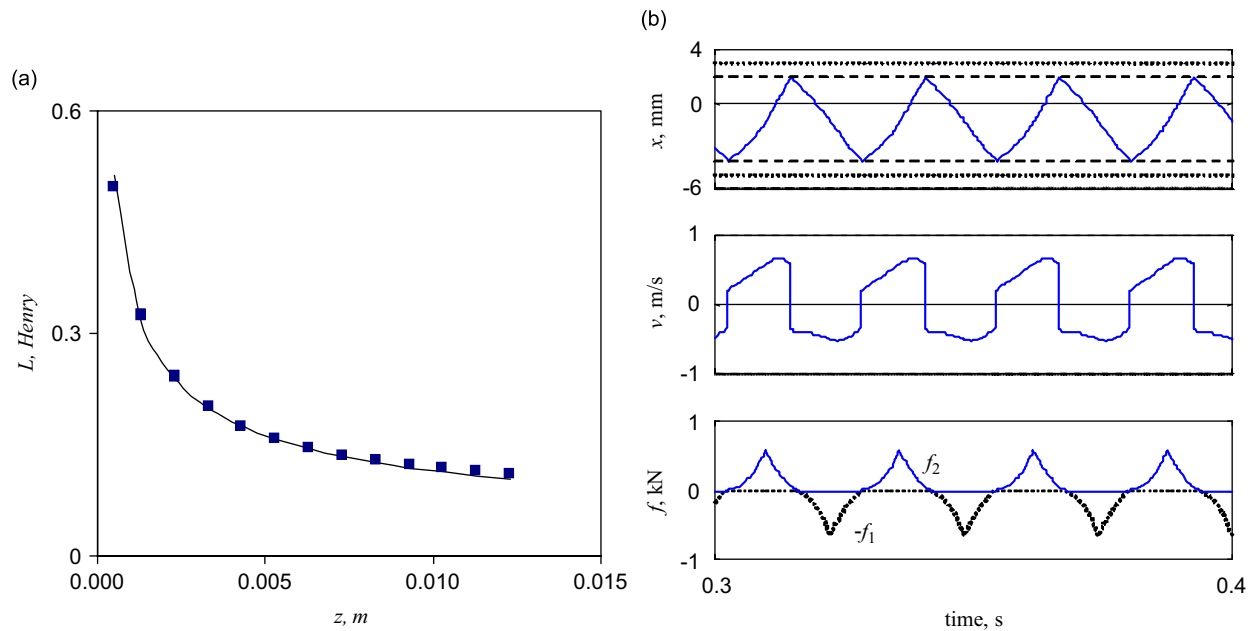


Fig. 15. Inductance characteristic (a) and vibration and force waveforms (b).

4.2. Simulation results

The following parameters of the mechanical system were used for simulation: $m = 10$ kg; $\omega_0 = \sqrt{c/m} = 2\pi \times 20$; $D = b/(2m\omega_0) = 0.1$, $r = 0.6$. The magnet inductance L dependence on the gap z was approximated by the function $L(z) = 0.0115/\sqrt{z}$ (Fig. 15(a)). The dark squares here show the experimentally obtained data for the real magnet.

Fig. 15(b) shows an example of the steady-state vibration with a frequency about 40 Hz and the excitation force waveforms. These curves are obtained for the value $U_c = 250$ V of the constant voltage and control corresponding to Fig. 11(a). The respective transient process of the vibration initiation is shown in Fig. 16. Here, projections of the 3D curve represent the time behaviour of displacement $x(t)$, velocity $v(t)$, and the phase-plane trajectory $v(x)$ with the limit cycle.

The steady-state excitation force is essentially polyharmonic (Fig. 15(b)) due to the saw-shape current waveform and quadratic current to force transformation (4). However its high harmonics hardly appear in the

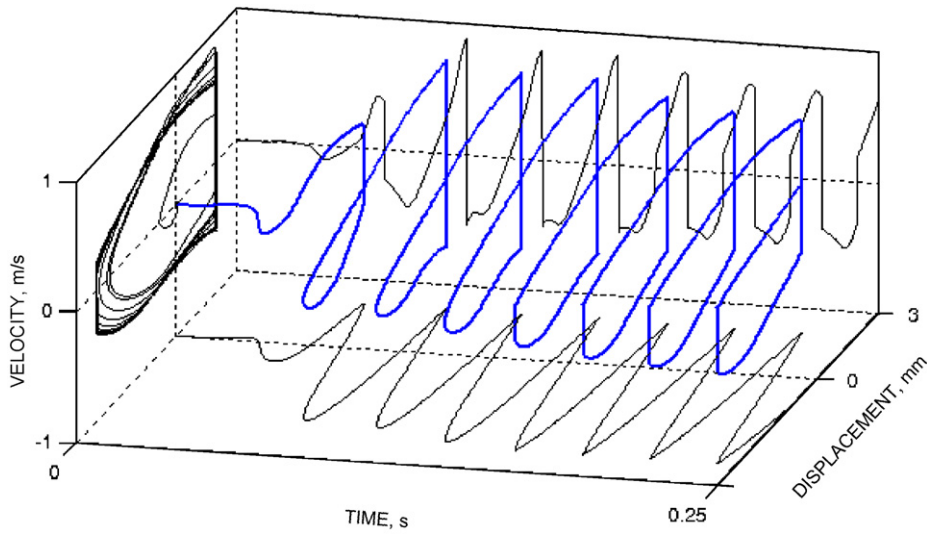


Fig. 16. Transient process of vibration initiation.

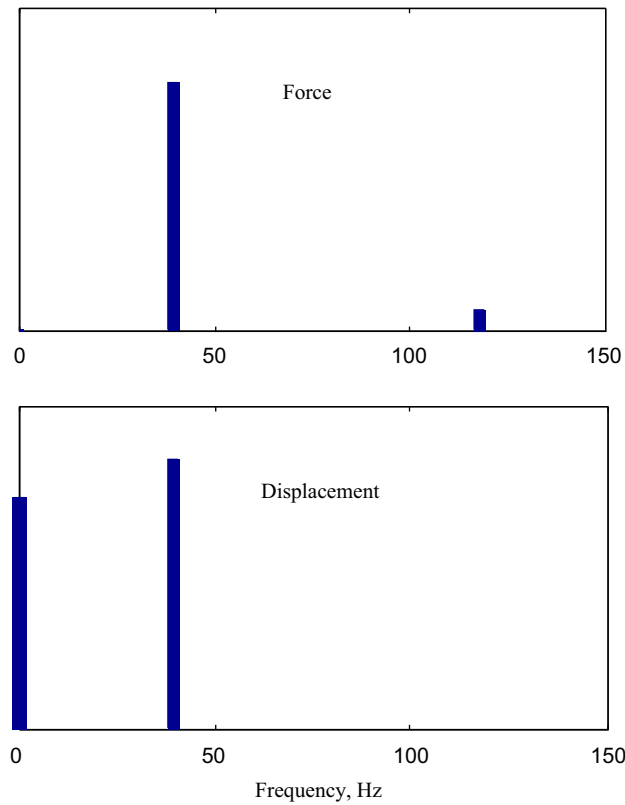


Fig. 17. FFT spectrums of force and vibration.

resulting vibration due to the near-resonant regime of vibration. Fig. 17 shows the FFT spectrums of the steady-state excitation force and of the resulting vibration. The constant component of the displacement (zero frequency) is the result of the asymmetric limiters.

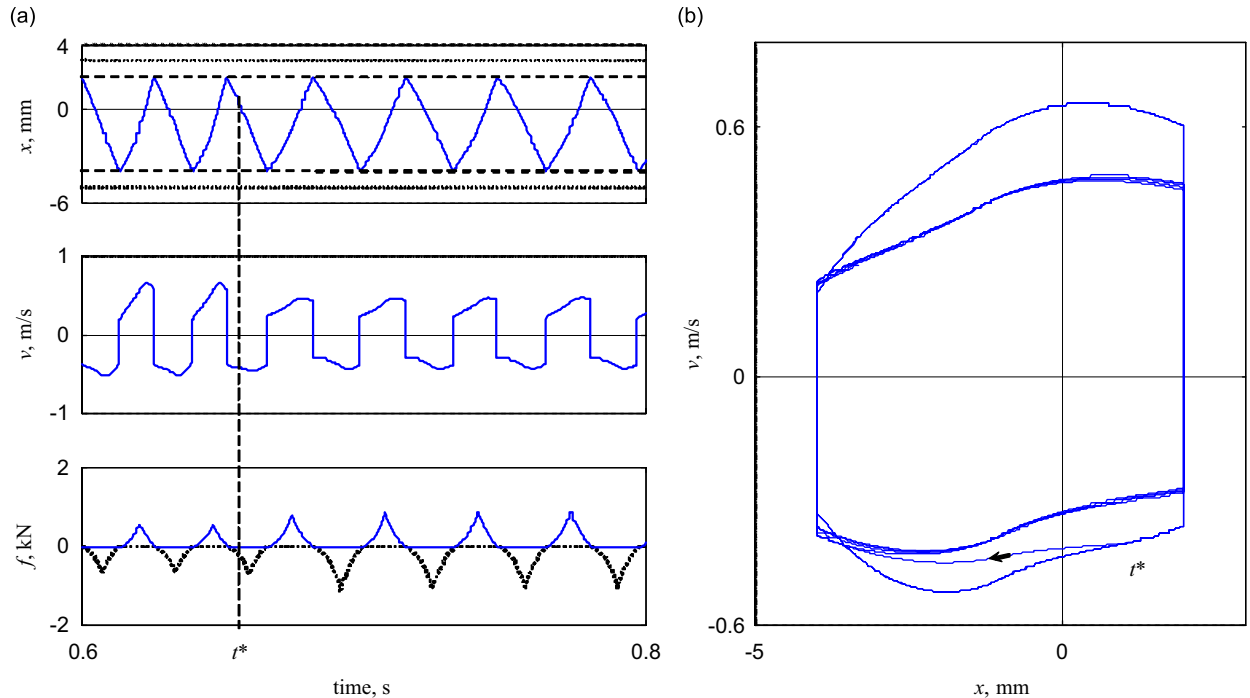


Fig. 18. System behaviour under changing load: time diagram (a) and phase-plane trajectory (b).

The system under consideration is very robust. It keeps the effective vibro-impact regime of vibration even under a wide unpredictable variation of parameters. Fig. 18(a) shows the system behaviour under a sudden triple increase in the vibrating mass m at the time instant $t = t^*$. The corresponding phase-plane trajectory is shown in Fig. 18(b). From this figures, we notice that the system keeps the stable regime of vibration with two impacts per a period while changing almost instantly the frequency of vibration. It moves to the new limit circle in the phase plane within one period of vibration. The corresponding control signal and electric currents change accordingly to Fig. 11(a).

It is clear from Fig. 15(b) that the steady-state regime of vibration is near-resonant. To investigate this regime more thoroughly we will compare it with other possible regimes of vibration. The following regimes are considered below:

- vibration under conventional forced excitation with variable frequency;
- autoresonant vibration under a small variation of the phase shift between the excitation force and vibration.

Forced excitation with frequency control: In this case, the switch S in Fig. 14 is used to open the autoresonant feedback circuit. The same switch inputs two independent external sinusoidal signals with equal regulated frequency to the 'Control' block. The above-described transformation (1) shown in Fig. 11(a) for $k = 0$ is used to form the control signal on the base of these external signals. In comparison with conventional frequency-regulated systems the system under consideration exhibits an unusual dependence of the excitation force amplitude on the frequency. In general, the force amplitude is proportional to the squared amplitude of the current (4), which is inversely proportional to the frequency. To avoid the high values of force (and current) at low frequencies of vibration under constant value of voltage supply the amplitude of current must be restricted. This can be achieved simply by limiting the duration of the control pulse. This limitation was chosen as 0.25×30 ms. As a result the amplitude of excitation force depends weakly on frequency when it is lower than 33 Hz and then decreases slowly at higher frequencies (including the above-mentioned frequency

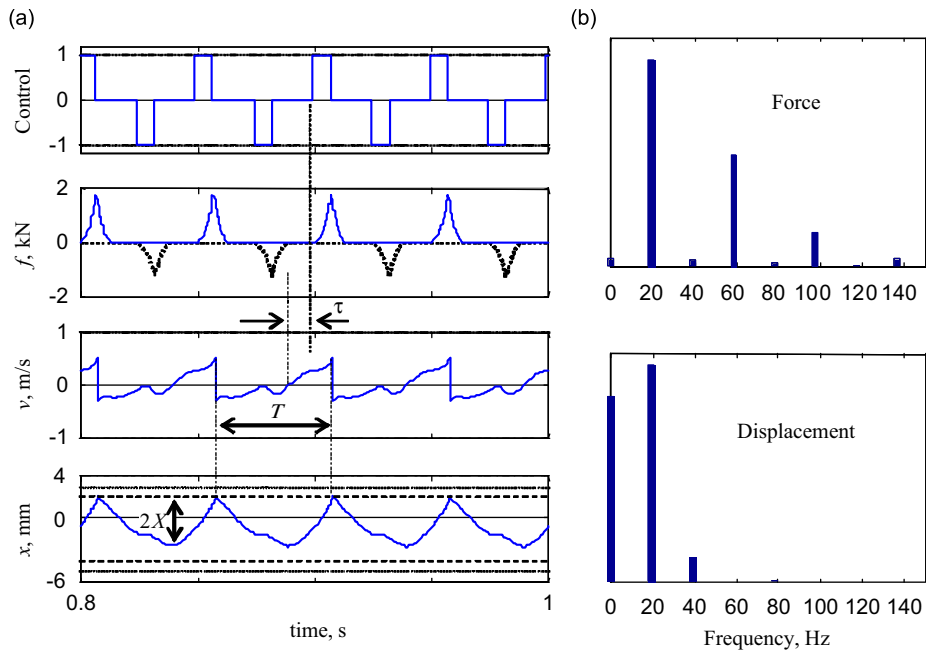


Fig. 19. Non-resonant vibration with one-sided impacts: waveforms (a) and FFT spectrums (b) of force and vibration.

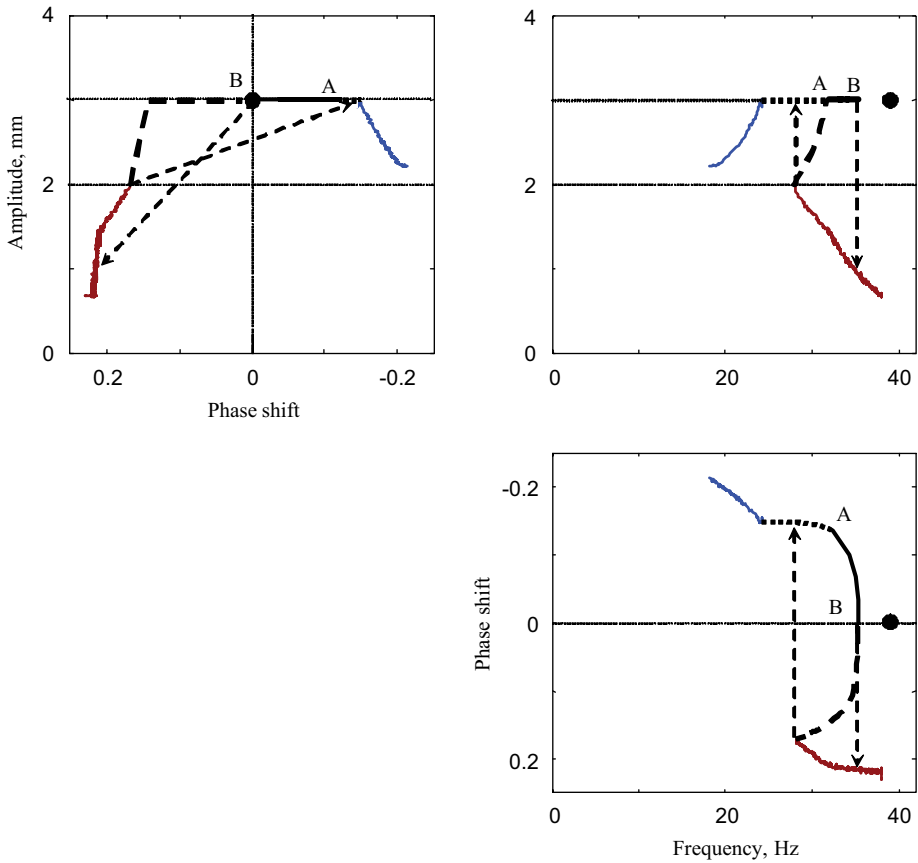


Fig. 20. Amplitude–frequency–phase curves for forced excitation.

40 Hz of the autoresonant vibration). Fig. 19(a) is an example of the waveforms for forced vibration with one-sided impacts at frequency 19.5 Hz. The excitation force f has now more pronounced high harmonics, as shown in Fig. 19(b), due to restriction of the control pulses length. The displacement waveform also has considerable second harmonics as a result of non-resonant regime of vibration.

The resulting amplitude–frequency, phase–frequency and amplitude–phase characteristics are shown in Fig. 20. These curves were obtained by slowly changing the frequency of excitation.

Half of the peak-to-peak value of vibration was used to present the amplitude X of vibration as shown in Fig. 19(a). The phase shift between the excitation force and the resulting vibration was estimated as τ/T , where T is the period of vibration and τ is the time lag between the control signal (voltage) and the resulting velocity of vibration as shown in Fig. 19(a). Autoresonant excitation corresponds to a zero value of the phase shift as shown in Fig. 11(a) and the phase shift in Fig. 19(a) is negative. The value $\tau/T = 0.25$ corresponds to conventional $\pi/4$ or 90° phase shift. Two horizontal thin lines on the amplitude–phase and amplitude–frequency plots of Fig. 20 indicate the amplitudes under which the vibro-impact regimes with one- and two-sided impacts period arise. The dotted parts of the bold curves correspond to irregular regimes of vibration with unsteady amplitude and a number of impacts during a period of excitation [7]. The dashed parts correspond to unstable regimes that cannot be obtained under forced excitation with frequency control. This instability results in two jumps shown with dashed arrows, which take place under slow increase and slow decrease in the excitation frequency. Only part ‘AB’ of the curves corresponds to stable periodic regimes with two impacts per period. However, these regimes cannot be used practically for two reasons. First, these regimes can be reached only under a slow increase of the excitation frequency. Otherwise, low-amplitude impact-free regimes arise. Second, jumps can occur from accidental disturbances resulting again in the low-amplitude regimes.

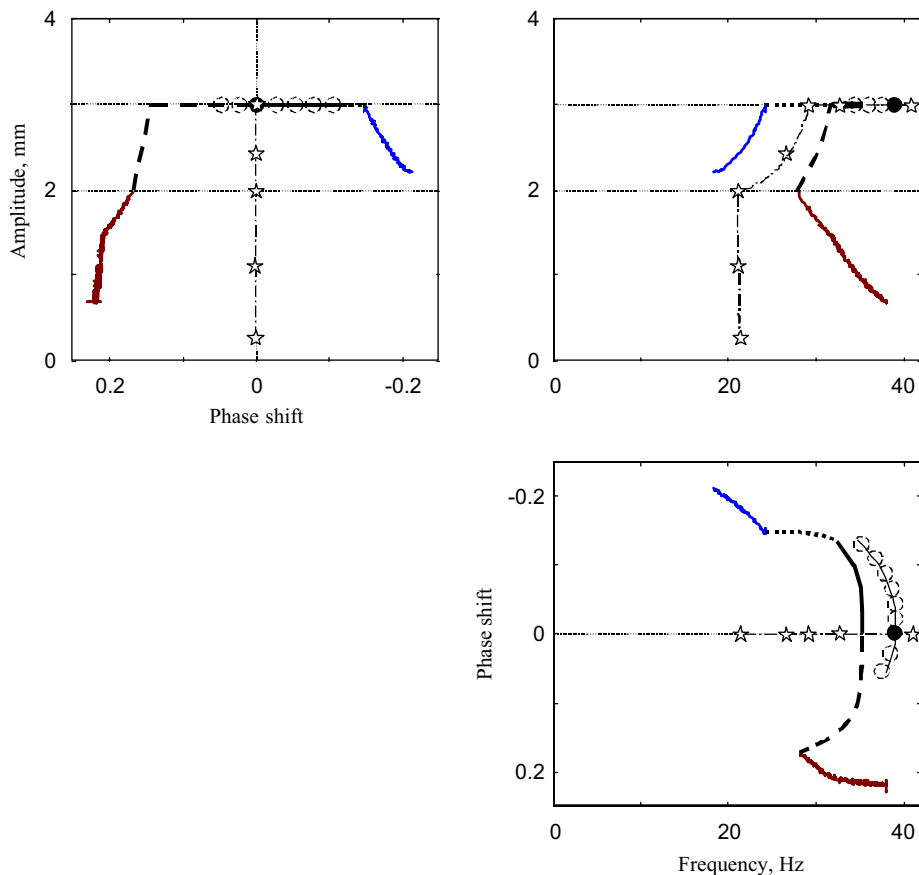


Fig. 21. Autoresonant excitation with phase control and amplitude control.

The small black circle in Fig. 20 defines the auto-resonant regime of vibration corresponding to the closed feedback circuit, as shown in Fig. 14. This regime is periodic (Figs. 15(b), 18) and stable. It self-excites instantly (Fig. 16) and is the only stable state of the autoresonant system. The autoresonant vibration slightly differs from the forced vibration corresponding to the point 'B'. This discrepancy is caused by a small difference in shape of the control signals (and force) formed from the real vibration signal and the ideal external sinusoidal signal.

The considered autoresonant system does not need any additional phase-shifting elements in the feedback circuit. However, it is interesting to investigate how far the obtained regime is from the most intensive one. To do this a phase control [8] was added to the model. The block 'Control' in Fig. 14 has the special input that allows for addition of a small phase shift into the feedback circuit. The parameters of self-sustained regimes obtained under small deviations of the phase shift are shown with white dashed circles in Fig. 21. These results show that the initial autoresonant regime of vibration (small black circle) is practically indistinguishable from the most intensive one with the maximum frequency. It is also important that, as predicted, even noticeable variations in the phase shift have only a small effect on resulting regime (frequency) of vibration.

Changing the magnitude of constant voltage U_c also allows the autoresonant regime of vibration to be controlled. The dash-dotted lines marked with stars in Fig. 21 show how parameters of the autoresonant regime change under slow variation of U_c in the 25–260 V range. It can be seen that resonant regimes with one-sided impacts or without impacts can be obtained in the autoresonant system, if necessary. Changing the on-off time ratio (relative pulse duration) of the control signal under constant U_c will result in approximately the same curve. This line almost exactly corresponds to the backbone [7] of the considered vibrating system. The backbone describes a relationship between amplitude and frequency of free vibration. When the autoresonant system is initially turned on, parameters of the developing vibration (Fig. 16) change approximately along this line.

5. Conclusions

An autoresonant approach enables intrinsic drawbacks in the use of electromagnetic actuators for vibrating and vibro-impact machines to be overcome. Elemental electromagnetic actuators can be successfully used in various autoresonant systems, including high-power vibrating machines. A simple and robust control system provides an efficient and stable resonant regime of vibration with impacts that cannot be used under traditional methods of excitation. This vibration mode is self-exciting, and the system maintains a resonant regime even under major changes in load. Resonant regimes with two-sided impacts, one-sided impacts or without impacts can be obtained.

References

- [1] I. Gutman, *Industrial Uses of Mechanical Vibrations*, Business Books Limited, London, 1968.
- [2] L.K. Brandt, B. Love, *Mud Equipment Manual, Handbook 3: Shale Shakers*, Gulf Publishing Company, Houston, 1982.
- [3] V. Astashev, V. Babitsky, M. Kolovsky, *Dynamics and Control of Machines*, Springer, Berlin, 2000.
- [4] V.I. Babitsky, Autoresonant mechatronic systems, *Mechatronics* 5 (1995) 483–495.
- [5] V. Kononenko, *Vibrating Systems with a Limited Power Supply*, Iliffe Books Ltd., London, 1969.
- [6] K. Magnus, *Vibrations*, Blackie & Son Limited, London, 1965.
- [7] V.I. Babitsky, *Theory of Vibro-Impact Systems and Applications*, Springer, Berlin, 1998.
- [8] I.J. Sokolov, V.I. Babitsky, Phase control of self-sustained vibration, *Journal of Sound and Vibration* 248 (2001) 725–744.
- [9] H.C. Roters, *Electromagnetic Devices*, Wiley, New York, 1963.